DOI: http://dx.doi.org/10.1590/2179-10742017v16i2822

Design of Microstrip Antenna Array with Suppressed Back Lobe

Eduardo S. Silveira, Daniel C. Nascimento, Alexis F. Tinoco-S.
Laboratory of Antennas and Propagation, Technological Institute of Aeronautics, São José dos Campos – SP, Brazil. E-mails: eduardosilveiranes@gmail.com, danielcn@ita.br, atinoco@ita.br
Marcus V. P. Pina
Integration and Testing Laboratory, Brazilian Institute of Space Research, São José dos Campos – SP, Brazil. E-mail: marcus.pina@lit.inpe.br

***Abstract*—A practical procedure to reduce the back lobe level of linear microstrip antenna arrays is presented in this paper. The novel concept consists in the design of the radiators asymmetrically positioned with respect to the ground plane. In order to validate this technique, a four-element linearly-polarized array is designed in the HFSS software and a prototype is manufactured. Furthermore, the design of beamforming circuit to achieve broadside radiation and -20 dB side lobe level is detailed. Very good agreement between simulated and experimental results is obtained. Although the technique is presented for linearly polarized arrays, it is general and can also be applied in the circularly polarized ones.**

***Index Terms*—** microstrip antenna arrays, beamforming circuit, back lobe suppression

I. INTRODUCTION

Microstrip antenna arrays are widely used in global navigation satellite systems (GNSS) and communication systems due to its low profile characteristic, conformability, lightweight and low cost [1]. These arrays, when composed by linearly polarized patches in side by side configuration [2], exhibit a high back lobe level [2]-[4] due to asymmetric E-plane radiation pattern [5]. This undesired behavior allows that multipath signal propagation remain a dominant cause of error in differential positioning system [6]. Also, it affects the coverage capacity of base station sectorial antenna, due to the overlapping areas between adjacent sectors [7].

The above-mentioned difficulties can be mitigated by using a low back lobe antenna. In the case of base station antennas array, FBR (front-back ratio) more than 20 dB is recommended in order to increase the subscriber capacity [7]. Various solutions for the improvement of FBR performance are available in the literature [6]-[14]. These solutions, based on technologies like that: electromagnetic bandgap (EBG), micromachining technology, substrate integrated waveguide (SIW), slotted ground choke, leaky-wave antenna, ground plane edge shaping and backed reflector behind the radiator, are efficient, but make manufacturing process more complex. The improvement of the FBR in a simple way is proposed in this paper, the solution is based on the antennas positioning with respect to the ground plane, thus making the manufacturing process simpler. This paper is structured as follow: In

Brazilian Microwave and Optoelectronics Society-SBMO received 25 Oct 2016; for review 27 Oct 2016; accepted 03 Jan 2017
Brazilian Society of Electromagnetism-SBMag *ISSN 2179-1074*

DOI: http://dx.doi.org/10.1590/2179-10742017v16i2822

the section II the back lobe radiation of a probe fed linear microstrip antenna array is presented as result of the asymmetric far field E-plane radiation pattern. In the sequence a technique based on the antenna positioning with respect of ground plane is carried out, reducing the undesired back lobe. This technique applied to a side by side array that makes the E-plane far field symmetric is assisted by a parametric simulation.

Section III describes a four-element side by side array design based on the prior studies. Special attention is given to the beamforming circuit design in section IV, to synthetize the excitation coefficients for a side lobe level of -20 dB. The section V shows the array prototype manufacturing and its experimental input impedance matching and radiation characteristics, compared with the theoretical ones. According [7] a FBR better than 20 dB is the goal of this work.

II. Back Lobe Analysis

Before starting the finite ground plane array design, a study of back lobe radiation becomes necessary for the better understanding of the back radiation mechanism. This undesired effect is treated in this work by the analysis of single antenna and two arrays printed in dielectric substrate of 2.55 relative permittivity and 3.048 mm thickness, both designed in HFSS software.

Firstly, a linearly-polarized single microstrip radiator is analyzed in HFSS software to elucidate the E-Plane asymmetries effect [5] and to provide elementary knowledge and skills for the array design. The analyzed antenna operating at 2.5 GHz (Fig. 1a) is a probe fed square microstrip patch of dimensions (35.0 mm×35.0 mm), printed atop of square dielectric substrate of dimensions (100.0 mm × 100.0 mm). Radiation patterns of E-plane (*xz*), and H-plane (*yz*), are presented in (Fig. 1b). The radiator operates in the fundamental mode (TM_{10}^{z}), taking the Fig. 1(a) as reference.

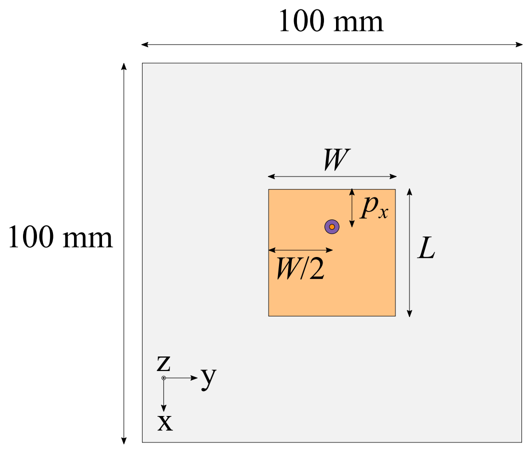

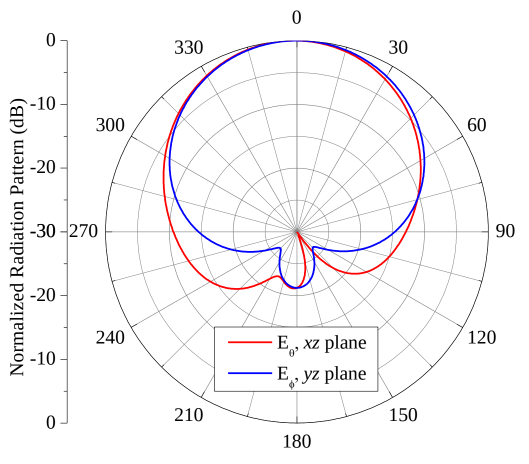

Fig. 1. (a) Single element microstrip antenna and its (b) E- and H-plane radiation patterns.

The E-plane radiation pattern of this radiator is indubitably asymmetric, enforcing a relevant field level in the back region. The asymmetric far field is attributable to the difference in phase between the fringes. This phenomenon is caused by the fact that probe excitation creates evanescent modes that

ISSN 2179-1074

DOI: http://dx.doi.org/10.1590/2179-10742017v16i2822

contributes to radiation pattern distortion [15]. This asymmetric shape in the E-plane is more pronounced for antennas printed in thicker substrates [16].

This undesired far field in the back region of a single element will create a high back lobe level when an array is composed. The back lobe behavior is next investigated in terms of the eight-elements arrays with half-wavelength spacing, in the side by side (Fig. 2) and collinear (Fig. 3) configurations. These arrays are designed in HFSS software and uniformly excited. Radiation pattern for both configurations are presented in Fig. 4. This figure illustrates that back lobe of side by side configuration is higher than collinear one. Depending on the electrical dimensions of ground plane and substrate thickness, the back lobe grows to unacceptable values [2], [16]-[17].

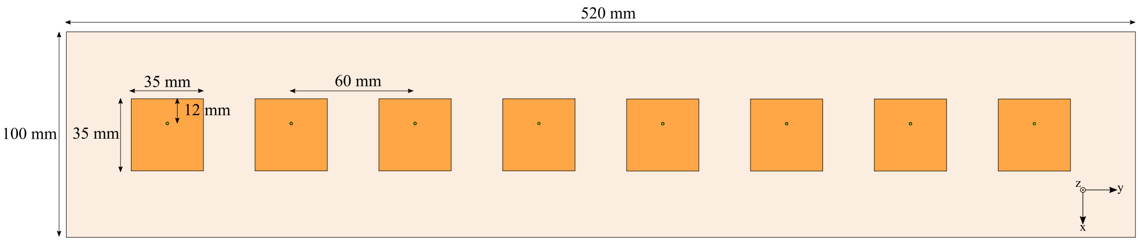

Fig. 2. Side by side array.

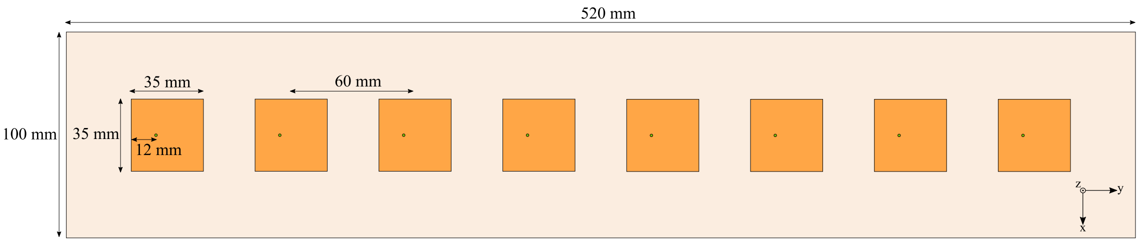

Fig. 3. Collinear array.

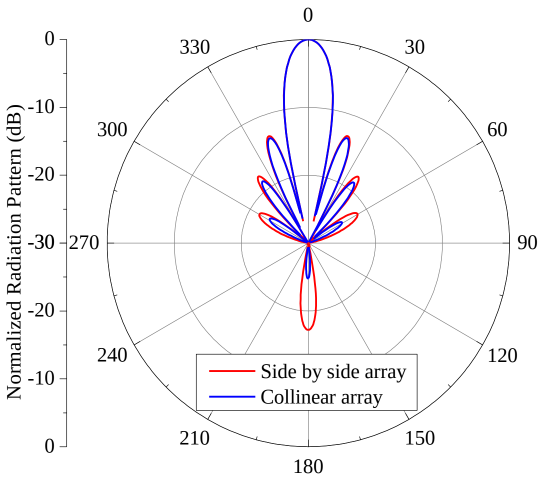

Fig. 4. Radiation pattern of uniformly excited arrays – yz plane.

An intuitive way to reduce the back lobe of side by side array is the compensation of fringing phase differences, making the E-plane radiation pattern symmetric and with a null at back lobe direction. In this work this compensation is realized by means of the border diffraction effects controlled by the

DOI: http://dx.doi.org/10.1590/2179-10742017v16i2822

radiators asymmetrically positioned with respect to the ground plane.

In order to get this condition, a back lobe level is investigated by a parametric analysis of relative positioning of the radiators with respect of the ground plane. This analysis is carried out, looking for the null of back lobe level that is achieved when the diffracted fields at ground plane border reach a condition that compensates the difference of the fringes phase.

The relative positioning of radiators above ground plane is established by variables (G_1, G_2, G_3, and G_4), in accordance with the dashed black and blue symmetry lines defined in the Fig. 5. Given the ground plane asymmetry variables, a parametric study was carried out and its results are shown as follows. During this study, each parameter was varied alone, while the rest were held fixed. The standard values for the parameters are: $G_1 = G_2 = 50$ mm and $G_3 = G_4 = 260$ mm. The influence of the variables G_1 and G_2 in the antenna array radiation pattern is shown in Fig. 6.

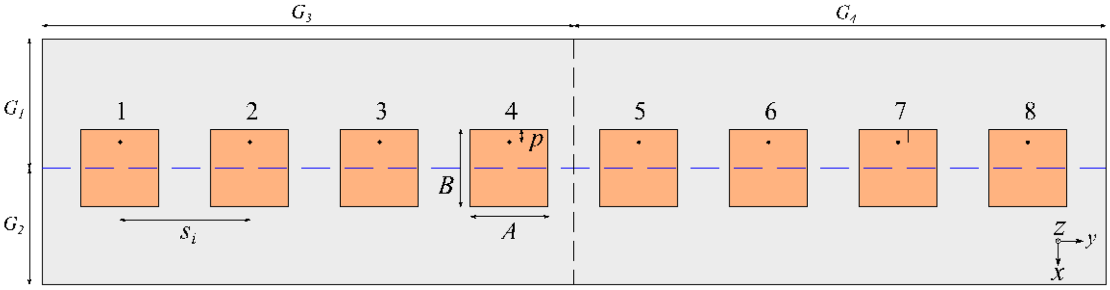

Fig. 5. Antenna array geometry.

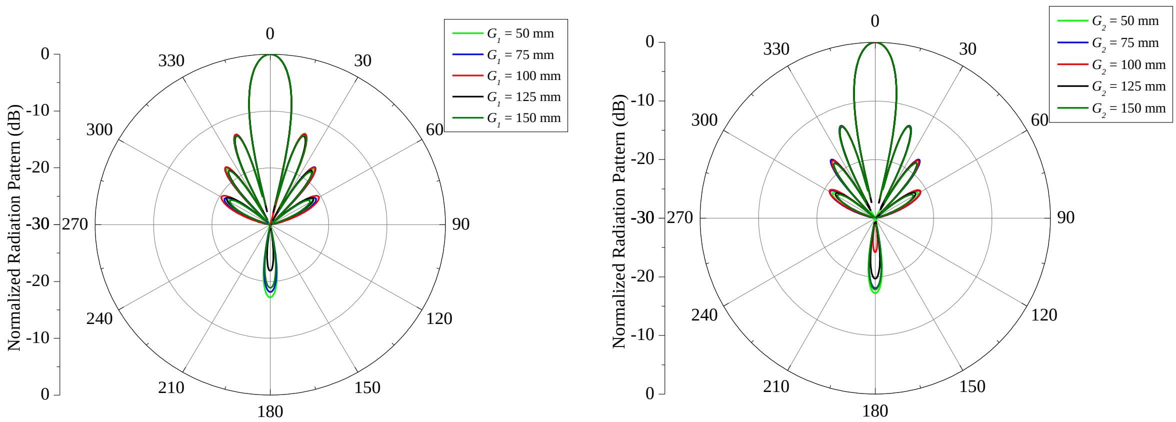

(a) (b)

Fig. 6. Antenna array total electric field for (a) G_1 and (b) G_2 variations – $\phi = 90^o$ plane.

From the parametric analysis it is clear that setting correctly G_1 and G_2 dimensions, the back lobe can be suppressed. To make evident the back lobe level reduction, the Tables 1 and 2 were built, synthetizing the data from the radiation patterns showed in Fig. 3 (a) and (b). On the other hand, in Fig. 7, the influence of G_3 and G_4 parameters, in the array back lobe is presented. One can observe that these parameters do not affect the array FBR.

DOI: http://dx.doi.org/10.1590/2179-10742017v16i2822

TABLE I. VARIATION OF THE BACK LOBE LEVEL (dB) WITH G_1 (mm).

G_1	Back Lobe Level
50	-17,21
75	-18,15
100	-28,91
125	-21,87
150	-18,88

TABLE II. VARIATION OF THE BACK LOBE LEVEL (dB) WITH G_2 (mm).

G_2	Back Lobe Level
50	-17,21
75	-18,05
100	-24,20
125	-19,68
150	-17,85

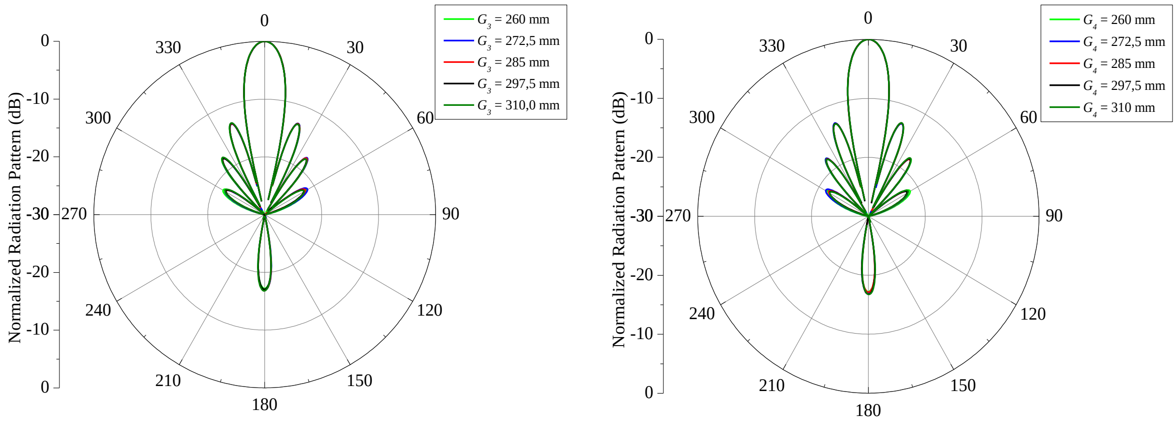

Fig. 7. Antenna array total electric field for (a) G_3 and (b) G_4 variations – ϕ = 90º plane.

III. ARRAY DESIGN

After detailing the back lobe level control process, the design of a four-elements array with half-wavelength spacing assisted by HFSS software is carried out, which allows a prototype to be built and tested. The array geometry is presented in Fig. 8. Using the Arlon CuClad 250-GX of 3.048 mm thickness, the array patches dimensions (A=B=35 mm) are established to provide an ISM 2.5 GHz operating frequency. The probe position p is set to 12 mm. The separation S_i between the elements is defined as 60 mm ($\lambda_0/2$). As previously exposed, the ground plane dimensions are (G_1 = 100 mm, G_2 = 50 mm, and G_3 = G_4 = 140 mm), to eliminate the back radiation. The antennas are excited with the following incident voltage wave coefficients [18] ($a_1 = a_4 = 0.64$ and $a_2 = a_3 = 1$), calculated by a least square linear constraints algorithm [19], establishing SLL (side lobe level) of -20 dB. The coefficients indexes are related to each array element, taking the Fig. 8 as reference. To illustrate the potential of this technique in the back lobe reduction, radiation patterns of the array with asymmetric (G_1 = 100

DOI: http://dx.doi.org/10.1590/2179-10742017v16i2822

mm and G_2 = 50 mm) and symmetric ($G_1 = G_2$) ground plane are shown in Fig. 9.

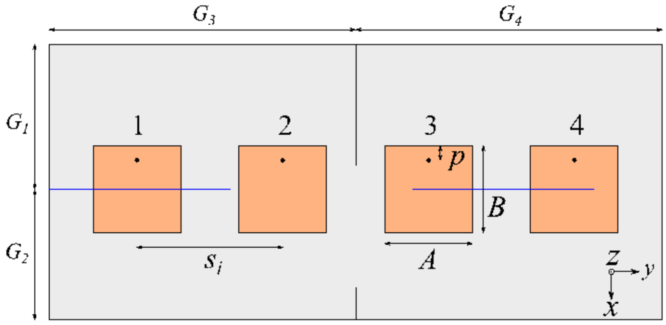

Fig. 8. Antenna array geometry.

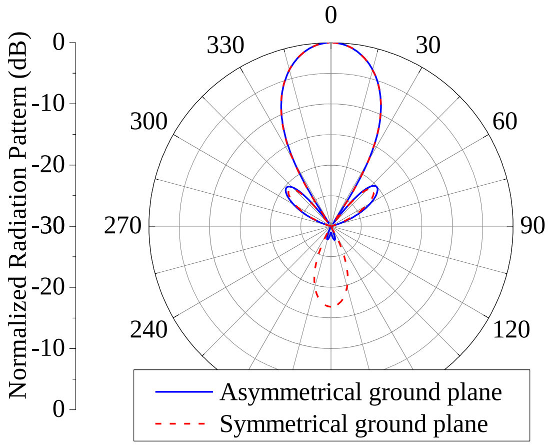

Fig. 9. Antenna array radiation patterns for symmetrical and asymmetrical ground planes – ϕ = 90º plane.

Finally, to validate the explanation above described with respect of asymmetric radiation pattern, the far field E-plane (*xz*-plane) of the array is plotted in Fig. 10 for the asymmetrical and symmetrical ground plane conditions. Using the correct asymmetrical ground plane dimensions, it is possible to observe the symmetric radiation pattern with a null at θ = 180º, responsible for the back lobe elimination. After the array project, the next step consists in the beamforming circuit design, presented below, contemplating the excitations above described.

  ISSN 2179-1074

DOI: http://dx.doi.org/10.1590/2179-10742017v16i2822

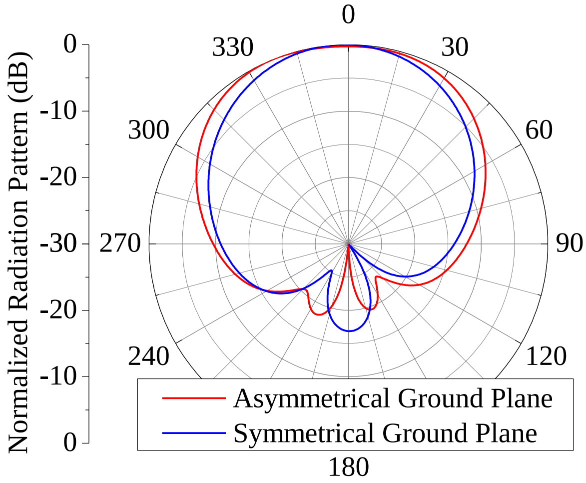

Fig. 10. Antenna array radiation patterns for symmetrical and asymmetrical ground planes – ϕ = 0º plane.

IV. Beamforming Circuit Design

The topology of the antenna array with beamforming circuit is a multilayer structure presented in the Fig. 11, where the circuit is positioned behind the antenna ground plane. The beamforming dielectric substrate is the TMM 4 of h_2 = 0.381 mm. An electrical thin substrate is employed in order to reduce microstrip circuit radiation. Note that, due to relative permittivity and dielectric thickness, the employed microstrip transmission line characteristic impedance (Z_0) is extremely low (values between 20 Ω and 50 Ω). This values are used to insure widths between 0.7 mm and 2.6 mm to designed transmission lines.

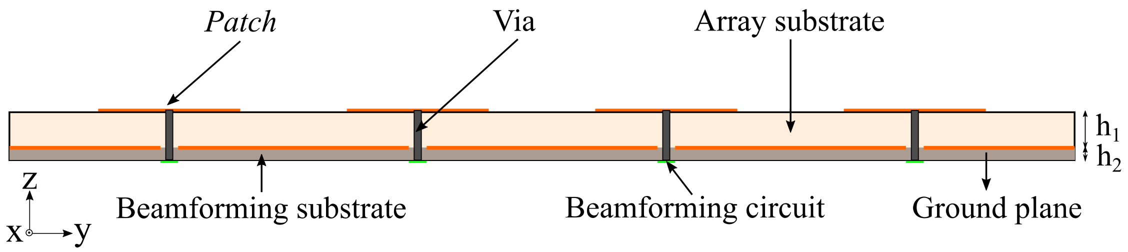

Fig. 11. The cross section of the array topology.

Having chosen the beamforming structure, the transition between the printed antenna and the beamforming circuit was designed following [2]. It is composed of a cylindrical probe (radius = 0.65 mm and length = 3.429 mm). Firstly, considering the aforementioned coefficients, the beamforming circuit was optimized for real active input impedance (Z_{in}) at the reference planes (RP) indicated in Fig. 12 (a). Furthermore, in Fig. 12 (b), the first set of quarter wave transformers are used to reduce the active terminals impedance (Z_{in} = 10Ω) as indicated.

  ISSN 2179-1074

DOI: http://dx.doi.org/10.1590/2179-10742017v16i2822

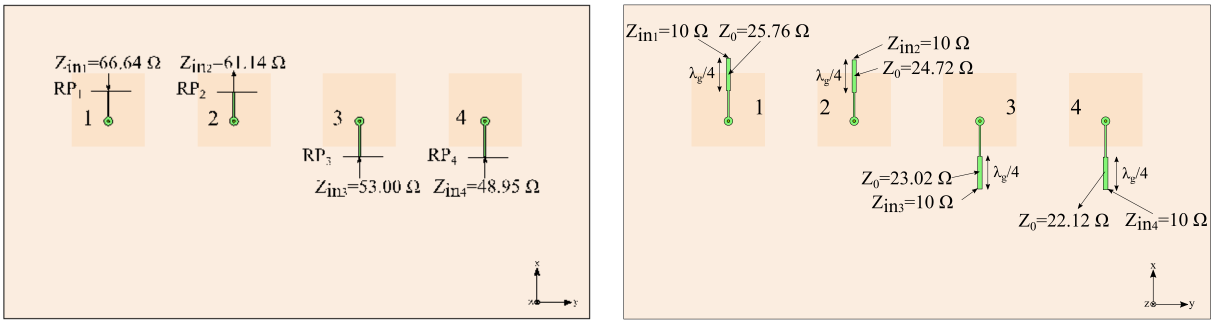

(a) (b)

Fig. 12. Definition of (a) reference planes (RPs) impedances and (b) first set of quarter wave transformers.

Next, a second set of quarter wave transformers are designed (see Fig. 13 (a)) to make physically possible the implementation of the T-junctions. The impedances of this second set of transformers were designed to provide the desired excitation coefficients, and to impose a 40-**Ω** of input impedance at the T-junctions as shown in Fig. 13 (b).

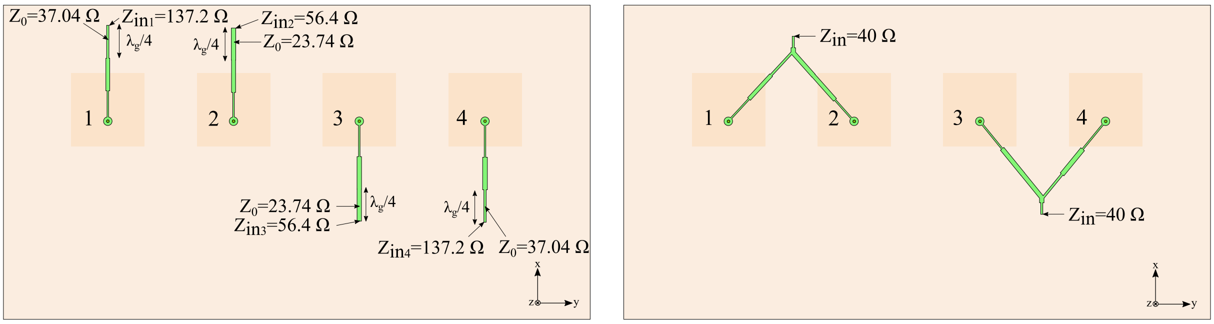

(a) (b)

Fig. 13. (a) Second set of quarter wave transformers and (b) connection of the terminals in T junctions.

The T-junctions input terminals were then extended by means of matched microstrip lines (40 **Ω**), as it is shown in Fig. 14 (a). Then, a novel T-junction was introduced to connect the two circuit sections, as it can be seen in Fig. 14 (b).

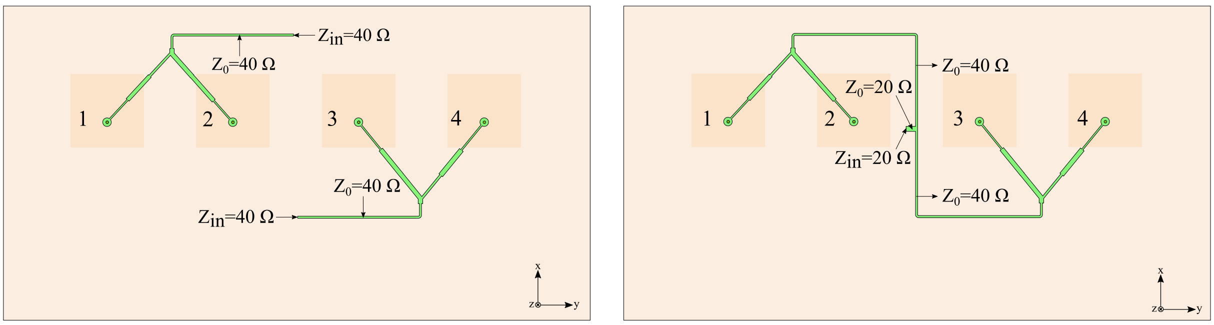

(a) (b)

Fig. 14. (a) Extension of the T junctions input terminals and (b) connection of the two circuit sections.

DOI: http://dx.doi.org/10.1590/2179-10742017v16i2822

Finally, the input terminal of the final T junction has its input impedance transformed to 50 Ω by a 32-Ω quarter wave transformer (see Fig. 15 (a)). A 50-Ω microstrip line is then used to extend the terminal connection up until the array edge (Fig. 15 (b)), allowing the inclusion of a SMA connector.

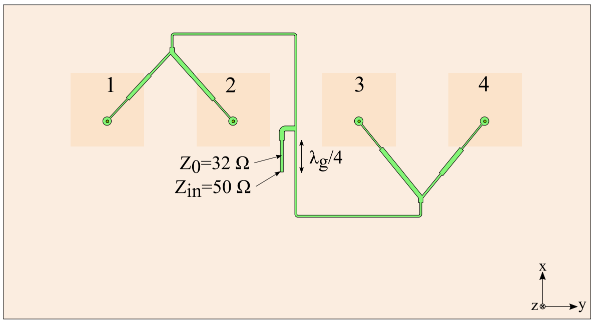

(a)

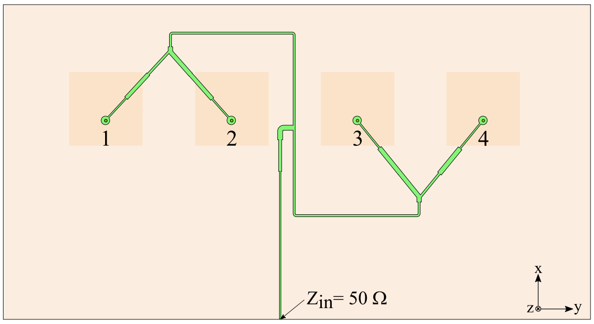

(b)

Fig. 15. (a) Inclusion of a final quarter wave transformer and (b) insertion of a 50-Ω microstrip line.

V. Array Prototype and Experimental Results

After the array (section III) and beamforming circuit (section IV) designs, a prototype was manufactured on LAP/ITA (Laboratory of Antennas and Propagation of Technological Institute of Aeronautics). The antenna array and beamforming circuit were manufactured using the T-Tech Quick Circuit AMC 2500. These two dielectric substrates were integrated using the Rogers 3001 bonding film. As this bonding film is a low loss dielectric, the antenna array ground plane had to be removed, imposing that the beamforming circuit ground plane works like antennas array ground plane simultaneously.

The beamforming circuit prototyped in the TMM substrate is presented in Fig. 16 (a) whereas the antenna array prototyped in the Arlon CuClad is presented in Fig. 16 (b). Note that, a copper-made bar was introduced in the structure (see Fig. 16 (b)), providing mechanical support to the 50-Ω SMA connector. Simulations of the array in the presence of this metallic support were carried out indicating that array works properly as previously expected.

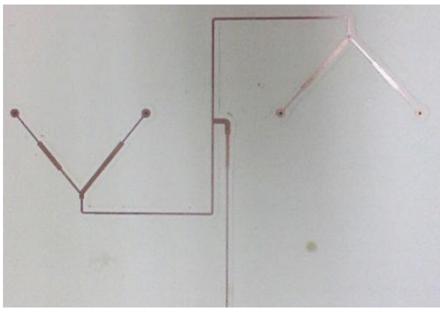

(a)

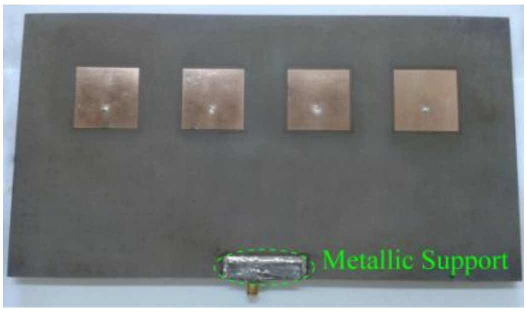

(b)

Fig. 16. Prototype of linearly polarized array: (a) – Beamforming circuit and (b) – Microstrip patches.

  ISSN 2179-1074

DOI: http://dx.doi.org/10.1590/2179-10742017v16i2822

The experimental VSWR (Voltage Standing Wave Ratio) from measurements with a VNA (Vector Network Analyzer) Agilent N5230A and the simulated one with HFSS are shown in Fig. 17. To conclude the analysis, the experimental and simulated radiation patterns in *zy*-plane are compared. The measurements were carried out in the anechoic chamber located at LIT-INPE (Integration and Testing Laboratory – Brazilian Institute of Space Research). The results for the *zy*-plane patterns are presented in Fig. 17 and show that SLL and back radiation are properly controlled under -20 dB, as specified. From these figures, it is found that theoretical and experimental results are in very good agreement.

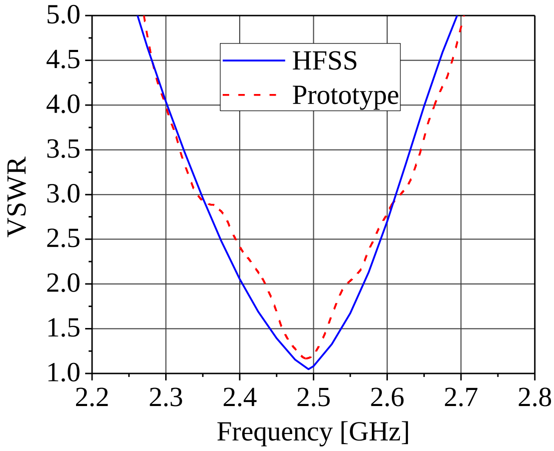

Fig. 17. VSWR of linearly polarized array.

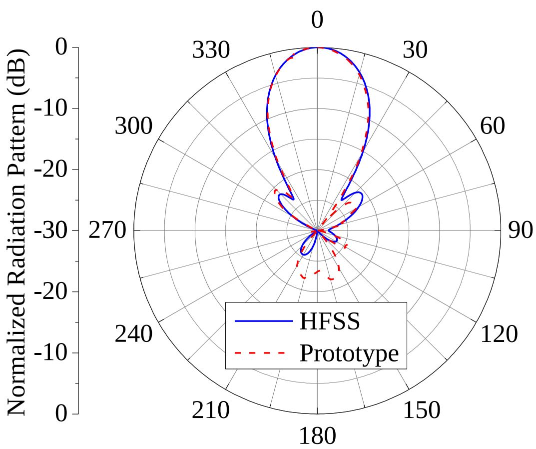

Fig. 18. Experimental and simulated normalized radiation patterns.

VI. Conclusion

This paper has shown a simple and easy-to-manufacture concept to reduce the back lobe level of microstrip antenna arrays. The proposed procedure is based on the asymmetrical disposal of the array elements with respect to the ground plane. A four-element linearly polarized antenna array was designed to verify the concept and special attention to its beamforming circuit design was given. Details about the beamforming circuit synthesis based on the active input impedance optimization were provided in a step-by-step approach. The FBR and SLL better than -20 dB was achieved in the experimental results, showing very good agreement with the simulated ones. The small discrepancies

DOI: http://dx.doi.org/10.1590/2179-10742017v16i2822

between prototype and theoretical results are certainly due to the inaccuracies in the construction processes, since it involves the bonding of the two substrates.

ACKNOWLEDGMENT

The authors would like to thank LIT/INPE for providing the use of the anechoic chamber and the Brazilian National Council for Scientific and Technological Development – CNPq, for the financial support of the projects 402017/2013-7, 131459/2014-7, and 141103/2016-7.

REFERENCES

[1] R. Garg, P. Bhartia, I. Bahl, A. Ittipiboon: "Microstrip Antenna Design Handbook", Norwood, MA: Artech House, 2001.
[2] D. C. Nascimento, J. C. da S. Lacava: "Design of Arrays of Linearly Polarized Patch Antennas on an FR4 Substrate: Design of a probe-fed electrically equivalent microstrip radiator", *IEEE Antennas and Propagation Magazine*, vol. 57, no. 4, pp. 12-22, 2015.
[3] Y. M. Yoon, J. H. Kim, B. G Kim: "Radiation characteristics of an H-plane linear microstrip array antenna on a finite substrate", 2013 IEEE Antennas and Propagation Society International Symposium (APSURSI), 2013.
[4] S. Farzaneh, A. R. Sebak: "Microwave Sampling Beamformer – Prototype Verification and Switch Design", *IEEE Trans. Microwave Theory and Techniques*, vol. 57, no. 1, pp. 36-44, Jan. 2009.
[5] T. Namiki, Y. Murayama, K. Ito: "Improving radiation-pattern distortion of a patch antenna having a finite ground plane", *IEEE Trans. Antennas Propagat.*, vol. 51, no. 3, pp. 478-482, 2003.
[6] W.-G. Lim, H.-s Jang, J.-W. Yu: "New Method for Back Lobe Suppression of Microstrip Patch Antenna for GPS", Proceedings of the 40th European Microwave Conference, Paris, France, September, 2010.
[7] Y. Rikuta, H. Arai, Y. Ebine: "Enhancement of FB Ratio for Cellular Base Station Antenna by Optimizing Reflector Shape", IEEE Antennas and Propagation Society International Symposium, Boston, USA, July, 2001, pp. 456-459, doi 10.1109/APS.2001.960133.
[8] L. Zhang, S. Gao, Q. Luo, P. R. Young, Q. Li, Y.-L Geng, R. A Abd-Alhameed: "Single-Feed Ultra-Wideband Circularly Polarized Antenna With Enhanced Front-to-Back Ratio", *IEEE Trans. Antennas Propag.*, vol. 64, no. 1, pp. 335-360, Jan. 2016.
[9] T. J. Cho, H. M. Lee: "Front-to-Back Ratio Improvement of a Microstrip Patch Antenna by Ground Plane Edge Shaping", 2010 IEEE Antennas and Propagation Society International Symposium, Toronto, ON, July, 2010, pp. 1-4, doi 10.1109/APS.2010.5561174.
[10] H.-m. Lee, J.-k. Kim: "Front-to-Back Ratio Improvement of a Microstrip Patch Antenna using an Isolated Soft Surface Structure", Proc. of the 39th European Microwave Conference, Rome, Italy, September, 2009.
[11] Y.-L. Chiou, J.-W. Wu, J.-H. Huang, C. F. Jou,: "Design of Short Microstrip Leaky-Wave Antenna With Suppressed Back Lobe and Increased Frequency Scanning Region", *IEEE Trans. Antennas Propag.*, vol. 57, no. 10, pp. 3329-3333, Oct. 2009.
[12] J. Wei, Z. N. Chen, X. Qing, J. Shi, J. Xu,: "Compact Substrate Integrated Waveguide Slot Antenna Array With Low Back Lobe", *IEEE Antennas Wireless Propag. Lett.*, vol. 12, 2013.
[13] M. Karami, R. A. Sadeghzadeh, M. Noferesti, M. Chegeni: "Suppressed back-lobe substrate-integrated waveguide slot array antenna for X-band", *IET Electron. Lett.*, vol. 51, no. 11, pp. 811-813, May 2015.
[14] Z. Aijaz, S. C. Shrivastava: "Techniques to Reduce the Back Lobe of Microstrip Slot Antenna", International Journal of Electronic Engineering Research, vol. 2, no.1, pp. 15-22, 2010.
[15] Ribeiro Filho, P. et al. "Probe-fed hybrid-patch cylindrical SIW antenna". 2014 IEEE Antennas and Propagation Society International Symposium (APSURSI), 2014.
[16] D.C. Nascimento. "Thick-substrate microstrip antenna arrays with beamsteering, side lobe level and directivity control". D. Sc. Thesis. Instituto Tecnológico de Aeronáutica, São José dos Campos, Brazil, 2013. (in Portuguese).
[17] M. Bonadiman. "Microstrip antenna array for airborne synthetic aperture radar". M. Sc. Thesis. Instituto Tecnológico de Aeronáutica, São José dos Campos, Brazil, 2004. (in Portuguese).
[18] D. M. Pozar: "The active element pattern": IEEE Transactions on Antennas And Propagation , v. 42, n. 8, p. 1176-1178, 1994.
[19] C. Y. Tseng, L. J. Griffiths: "A simple algorithm to achieve desired patterns for arbitrary arrays": *IEEE Trans. Signal Processing*, vol. 40, pp. 2737-2746, Nov. 1992.